SRTTU
Journal of Computational and Applied Research in Mechanical Engineering
jcarme.sru.ac.ir
JCARME
ISSN: 2228-7922

Research paper

Fatigue analysis of CRH2 high speed train railway wheels occurred due to random parameters

Mazuri Erasto Lutema[a,*] and Awel Mohammedseid Momhur[b]

[a]*Faculty of Transport Engineering and Technology, National Institute of Transport, Dar es Salaam, Tanzania*
[b]*African Railway Center of Excellence, Addis Ababa University, Addis Ababa, Ethiopia*

Article info:

Article history:

Received:	17/04/2023
Revised:	23/10/2023
Accepted:	26/10/2023
Online:	29/10/2023

Keywords:

Fatigue life,
Railway wheels,
Random parameters,
Finite element method,
Dynamic analysis.

[*]Corresponding author:
mazuri.erasto@nit.ac.tz
mazurilutema@yahoo.com

Abstract

The most crucial parts that literally sustain the safety of railroad rolling stock from the subfloor are the wheels. However, during operation, several random parameters can impair their performance, resulting in the train's unsafety. These unpredictable characteristics can lead to fatigue failure, especially in a CHR2 high-speed train. This study aims to analyse the fatigue life of railway wheels for the CHR2 high-speed train due to different random parameters. Three scenarios with random parameters were considered: suspension system, passenger weight, and train speed. A 3D wheel model created by CAD and analyzed with finite element software ANSYS and nCode to validate the model by applying static force. A railway vehicle-track dynamics was modeled with a 30t axle load using the vehicle-track dynamics theory. Then Monte Carlo simulations were performed to produce random samples of sensitive parameters and analyze their effect distributions on wheel–rail contact under random wheel parameters. The findings demonstrate that the random parameters of the suspension system have more negative effects on fatigue life compared to random passengers' weight and train speed; however, random passengers' weight has a less negative impact compared to random suspension and passenger weight. The dynamic stress analysis results showed that the random suspension system parameters have a high maximum stress compared to that obtained from random passengers' weight and train speed. Moreover, the random suspension system parameters have high maximum stress compared to that obtained from random passengers' weight and train speed.

1. Introduction

Railway wheels are among the most essential components of high-speed trains in terms of safety and performance. In recent years, the development of railway transport towards overload and high-speed operations has indeed led to significant advancements in locomotive technology. High-power locomotives have become increasingly prominent in this area, allowing for more efficient and faster rail transportation. However, wheels must withstand static, dynamic, and lateral loads while maintaining durability and safety, even in challenging environments [1, 2].

Fatigue failure is one of the main causes of failure in engineering and mechanical systems. Under cyclic loading, if the component reaches or exceeds the material fatigue limit, this will result in fatigue failure [3]. The number of cycles of a material or part in the event of damage is the life of the material or part [4, 5]. Fatigue damage in railway wheel systems is a significant concern, especially with the increasing volume of traffic and efforts to improve railway speeds. This issue is a critical consideration for ensuring the reliability and extended working life of key components in the wheel system [3, 6]. The two key product performances are safety and working life, which is a significant manifestation. [7]. These two factors have a direct impact on the wheel system reliability. Therefore, Railway engineers have already paid close attention to the fatigue parameters of the wheel system [2, 8, 9].

Higher train speeds with increasing axle weights and random characteristics, have resulted in higher wheel/rail contact forces [10, 11]. When the rolling speed is slow, the lateral movements concentrate at the zero-tracking center location. However, at a certain greater speed, the railway wheels lose their stability and declare their instability of motion [12]. Additionally, attempts have been undertaken to optimize wheel and rail design in order to improve performance while lowering costs. These developments have shifted the primary cause of tire rim degradation from wear to fatigue [13, 14]. Unlike the long deteriorating process of wear, fatigue results in abrupt fractures in wheels or material loss on the tread surface [15-18]. These failures may result in rail damage, suspension damage, and, in certain situations, major train disaster. Railroad wheel fatigue is sometimes referred to rolling contact fatigue, which is caused by repeated contact stress during the rolling action. Similar fatigue issues exist in other mechanical components that experience rolling contact loads, such as gears and bearings [19-22]. No current study investigated clearly the effect of random parameters on the wheels of CHR2 high speed by analysis fatigue life of the wheel. In this presented study, three scenarios with random parameters were considered: suspension system, passenger weight, and train speed, to analyze their fatigue life effect on the wheel of a CHR2 high-speed train.

2. Materials and methods

A 3D wheel model was created by CAD and analyzed by finite element software ANSYS and nCode to validate the model by applying static force. A railway vehicle-track dynamics model with a 30t axle load was developed using the vehicle-track dynamics theory. Then, random samples of sensitive parameters were generated using Monte Carlo simulations, and the distributions of their effects on wheel-rail contact for a set of arbitrary wheel parameters were assessed. Fatigue life of the wheel was then examined using the nCode after examination of the stress and total deformation, and major stress using maximum forces from the dynamic response.

2.1. Wheel railway model

The 3D wheel of high-speed train, shown on Fig. 1, was modelled by CAD, and the structural analysis of static force was done by ANSYS and nCode to obtain stress and fatigue life cycles. Using Manson-Coffin equation, as shown by Eq. (1) [23], the model was validated by comparing the results of static analysis life cycles and calculated life cycles. The latter for the wheel obtained 2.4045×10^{16}, which was not more differ from finite element life cycles results (3.005×10^{10}), implying it is safe to operate a high-speed train. Also, according to [24-27], the static stress obtained was compared to current research to validate the model and results obtained.

$$\sigma_{\max}\times\frac{\delta\varepsilon}{2}=\frac{(\sigma_f{}')^2\times(2N_f)^{2b}}{E}+\sigma_f{}'\times\varepsilon_f{}'\times(2N_f)^{b+c} \quad (1)$$

where, $\sigma_{\max}$ is the maximum stress, $\delta\varepsilon$ is the maximum normal strain, $\sigma_f{}'$ is the stress, N_f is the fatigue life cycles, E is the young modulus, $\varepsilon_f{}'$ is the strain, b and c are constants. The mechanical properties of the wheelset are shown in Table 1.

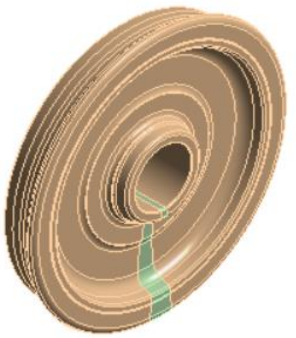

Fig. 1. Geometry of wheel.

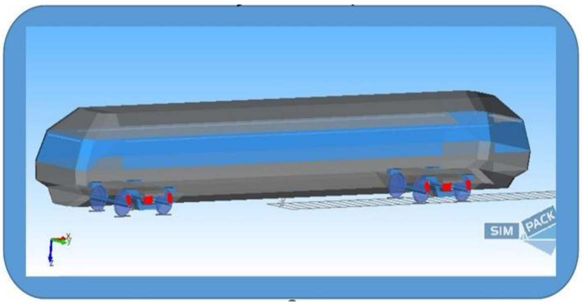

Fig. 2. Multibody model of rail vehicle.

2.2. Modelling of vehicle-multibody dynamics

The railway vehicle multibody dynamic model is composed of the submodels for the car, track, and wheel/rail interaction as shown in the Fig. 2. For each of the three categories, the current research created a multibody 3D dynamic model [5, 28]. A model of the CRH2 high-speed train with a 30-t axle load was created to investigate the wheel fatigue characteristics of a high-speed train-track system under uncertainty parameters. The vehicle's equation of dynamic motion can be expressed as a submatrix using the finite element method and vehicle-track connection in Eq. (2) [29].

$$M_V\ddot{D}_V + C_V\dot{D}_V + K_V D_V = P_{vt} \tag{2}$$

where $\ddot{D}_V$, $\dot{D}_V$, and D_V are the vectors of acceleration, velocity, and displacement of the vehicle subsystem, respectively. . The subscript V means the vehicle dynamics and track of the subsystem. M_V, C_V, K_V, and P_{vt} are the subsystem matrices of mass, stiffness, damping, and external force, respectively. The 3D model of wheelset and rail vehicle were modelled by Solidwork and Simpack, respectively. The parameters for high-speed railway vehicle are tabulated in Table 2.

Table 1. Wheelset mechanical properties [30].

	Type	Modulus	σ_f'	σ_f'	Poisson ratio	Density
Wheelset	ER8	210GPa	840	0.304	0.3	7500 kg/m^3

Table 2. CRH2 high speed trains mean parameters used in current research [29, 31].

Parameter	Notation	Value	Unit
Car body mass	m_c	35067	kg
Car body roll moment of the inertia	J_{cx}	119200	kg.m^2
Car body pitch moment of the inertia	J_{cy}	1711800	kg.m^2
Car body yaw moment of the inertia	J_{cz}	1615300	kg.m^2
Frame mass	m_t	3630	kg
Frame roll moment of the inertia	J_{tx}	2940	kg.m^2
Frame pitch moment of the inertia	J_{ty}	1990	kg.m^2
Frame yaw moment of the inertia	J_{tz}	3630	kg.m^2
Wheelset mass	m_w	1794	kg
Wheelset roll moment of the inertia	J_{wx}	900	kg.m^2
Wheelset pitch moment of the inertia	J_{wy}	220	kg.m^2
Wheelset yaw moment of the inertia	J_{wz}	950	kg.m^2
Vertical stiffness of the primary suspension per axle side	k_{pz}	980k	N/m
Lateral damping of the primary suspension per axle side	c_{py}	5490	kNs/m
Lateral stiffness of the primary suspension per axle side	k_{py}	1176000	N/m
Vertical damping of the secondary suspension	c_{pz}	20	kNs/m
Lateral stiffness of the secondary suspension per bogie side	k_{sy}	192	kN/m
Lateral damping of the secondary suspension per bogie side	c_{sy}	60	kNs/m

2.3. Model simulation

Monte Carlo simulation is indeed a powerful technique for dealing with uncertainty and variability in various processes, including those involving complex systems like railway operations [32-34]. Weibull equation was used for three parameters as Eq. (3) [29];

$$f(t)=\frac{\beta}{\eta}\times\left(\frac{t-\gamma}{\eta}\right)^{\beta-1}\times e^{\left(\frac{t-\gamma}{\eta}\right)\beta} \quad (3)$$

2.4. Random parameter selection for the vehicle-track dynamics system

The wheel-rail force in a train system is influenced by a wide range of factors such as train speed, suspension stiffness, passenger weight, wheel profile, railway track irregularity and track stiffness [5, 35-37]. Many of the variables affecting wheel-rail forces in a railway system are subject to chance and can be unpredictable to some extent. In this study, three scenarios for random parameters were considered, i.e., suspension system, passenger weight, and train speed. Tables 3–5 show the random parameter values for all situations. Considering random parameters in suspension systems, passenger weight, and train speed is crucial for safety, comfort, efficiency, and the overall performance of rail transportation systems. It enables engineers and operators to design and operate trains in handling a wide range of conditions while maintaining safety and reliability.

2.5. Formation of the stochastic parameters

It is uncertain what kind of random parameter distribution used in the vehicle-track dynamics system. Most parameters have a normal statistical distribution in various fields [17, 38]. In this study, it was assumed that the probability distribution of the random parameters influencing wheel-rail force follows a normal distribution. Monte Carlo simulations were used to get random number samples with a normal distribution, but first it solved two essential difficulties [5] of defining the sampling method used to produce a known distribution of random variables and calculating the random sampling sample size N. Eqs. (4-9) was used;

The generation of random numbers [23]:
The equation used for the multiplicative congruence method is;

$$x_{i+1} = (ax_i + c)\ (\mathrm{mod}\ m) \quad (4)$$

Eq. (4) shows the congruence of modulus m, and x_{i+1} is the reminder of (ax_i + c) divided by m. While a, c and m are positive integers. In the actual calculation, the parameter is introduced into the equation,

$$k_i = \mathrm{Int}\left(\frac{ax_i+c}{m}\right) \quad (5)$$

where Int is round numbers notation, and Eq. (4) becomes:

$$x_{i+1} = ax_i + c - mk_i \quad (6)$$

Table 3. Random of passenger's weight as case 1.

Parameter	Mean value	Std	Upper limit	Lower limit	Error	Units
Passenger weight	8	10%	8.3	7.7	3%	tons

Table 4. Random suspension system parameters as case 2.

Parameter	Mean value	Std	Upper limit	Lower limit	Error	Units
Vertical stiffness of primary the suspension/ axle side	980	10%	980.03	979.97	3%	kN/m
Lateral damping of primary s the suspension/ axle side	5490	10%	5520	5460	3%	kNs/m
Vertical stiffness of primary the suspension/ axle side	1176	10%	1176.03	1175.97	3%	kN/m
Vertical damping of the secondary suspension	20	10%	50	-10	3%	kNs/m
Lateral stiffness of the secondary suspension per bogie	192	10%	222	162	3%	kN/m
Lateral damping of the secondary suspension per bogie	60	10%	90	30	3%	kNs/m
Vertical stiffness of the secondary suspension per bogie	990.8	10%	1020.8	960.8	3%	kN/m
Vertical damping of secondary suspension per bogie side	9.8	10%	39.8	-20.2	3%	kNs/m

Table 5. Random train speed as case 3.

Parameter	Mean value	Std	Upper limit	Lower limit	Error	Units
Train speed	325	10%	350	300	3%	km/h

By dividing x_{i+1} by modulus m, the standardized random number will be as:

$$u_{i+1} = \frac{xi+1}{m} \tag{7}$$

By repeating the above approach, a set of random different numbers within the range (0, 1) can be obtained.

2.5. Random parameters of normal distribution formation [23]

It has been assumed that u_n and u_{n+1} are the two uniform random numbers within the interval (0,1). It adopts the following transformation to obtain two random numbers, $\mathring{x}_n$ and $\mathring{x}_{n+1}$; both obeys the standard normal distribution N (0.1);

$$\begin{Bmatrix} \mathring{x}_n & = (-2\ln u_n)^{\frac{1}{2}} \cos(2\pi u_{n+1}), \\ \mathring{x}_{n+1} & = (-2\ln u_n)^{\frac{1}{2}} \sin(2\pi u_{n+1}) \end{Bmatrix} \tag{8}$$

If random variable X obeys normal distribution N (m_x, σ_x), then its random numbers of x_n and x_{n+1} can be obtained using the following equations:

$$\begin{Bmatrix} x_n & = \mathring{x}_n \sigma_x + m_x \\ x_{n+1} & = \mathring{x}_{n+1} \sigma_x + m_x \end{Bmatrix} \tag{9}$$

3. Static force calculation

The strength of the Power bogie frame that comprises wheel was examined using the Power bogie frame's strength test method (TB/T2368-2005) [39] to comprehensively analyze the stress condition of the structure. it is imperative to calculate both the vertical and transverse loads. This approach allows for a more thorough assessment of the structural integrity and performance under different loading conditions.

3.1. Vertical load applied to the wheels

Based on the assumption of vehicles with mass evenly distributed among the eight (8) wheels and the body that is supported on each side frame of the bogie, Eqs. (10, 11) utilized for analysis and calculations.

$$F_y = [M_c + 2M_b + 4M_w] \times g \tag{10}$$

where;
M_c – Weight of car body = 35067 kg
M_b- Weight of bogie = 3630 kg
M_w- Weight of wheelset = 1794 kg
g- Acceleration due to gravity = 9.81 m/s^2
$F_y = [35067 + 2 \times 3630 + 4 \times 1794] \times 9.81$
$F_z = 485624.43$N

For vertical load applied to each wheel of the vehicle:

$$F_{y\text{-wheel}} = \frac{F_y}{8} \tag{11}$$

$$F_{y\text{-wheel}} = \frac{485624.43\text{N}}{8} = 60703.0538\text{N}$$

$$F_{y\text{-wheel}} = 60703.0538\text{N}$$

3.2. Hertz contact theory mathematical equation

It is critical to measure the accurate stress analysis for rail-wheel in order to predict the fatigue of wheels. In general, the Hertz contact theory is important for predicting rolling contact stress; however, this method has less accuracy for rolling contact stress results when a large number of stresses were developed [38], and Eqs. (12-16) were used. To calculate a number of contact areas and pressure distributions, it is necessary to understand the main formula by Hertz theory [40]. Kim [40] stated that the Hertz contact theory takes the radius of curvature of the rail and wheel profiles in contact as a constant and assumes no plastic deformation in the contact area. Fig. 3 depicts an elliptical rail-wheel contact with labeled dimensions x, y, z.

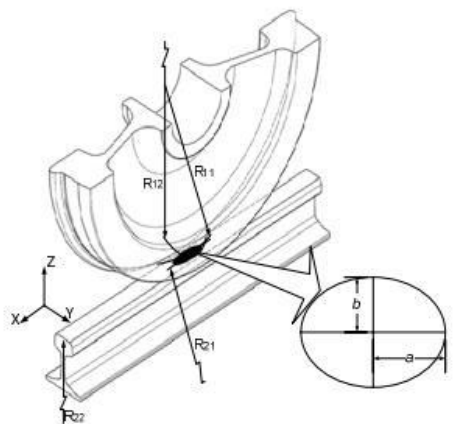

Fig. 3. Rail-wheel contact of elliptical [38].

To find the value of the normal pressure distribution p(x,y), Eqs. (12-14) can be used [41-43]:

$$P = p_0 \sqrt{\left(1 - \frac{x^2}{a^2} - \frac{y^2}{b^2}\right)} \tag{12}$$

a-x are the longitudinal direction for half-length width contacts area and b-y are the lateral direction half width contact area.

$$a = m\left(\frac{3\pi}{4} \times p\frac{K_1+K_2}{(A+B)}\right)^{\frac{1}{3}} \tag{13}$$

$$b = n\left(\frac{3\pi}{4} \times p\frac{K_1+K_2}{(A+B)}\right)^{\frac{1}{3}} \tag{14}$$

$$A+B = 0.5 \times \left(\frac{1}{R_{11}}+\frac{1}{R_{12}}+\frac{1}{R_{22}}+\frac{1}{R_{21}}\right) \tag{15}$$

While the difference of A and B obtained as;

$$B-A = 0.5 \times [(X+Y) \times cos2\beta]^{\frac{1}{2}} \tag{16}$$

where

$X = \left(\frac{1}{R_{11}} - \frac{1}{R_{12}}\right)^2 + \left(\frac{1}{R_{22}} - \frac{1}{R_{21}}\right)^2$ and

$Y = \left(\frac{1}{R_{11}} - \frac{1}{R_{12}}\right)\left(\frac{1}{R_{22}} - \frac{1}{R_{21}}\right)^2$

4. Results and discussion

The results presented in this study were acquired through mathematical calculations, dynamic simulations, and numerical simulations.

4.1. Dynamic response

Three cases of dynamic response were considered, the following maximum vertical wheel force results were obtained and shown in Figs. 4-6, which correspond to passengers weight for case 1, suspension system for case 2 and train speed for case 3, respectively.
To compute the rail-wheel contact areas, it is necessary to acquire the actual measurement of geometric constants for use in the above mathematics formula. The followings are the curve combinations; Eqs. (15, 16) [41-43];

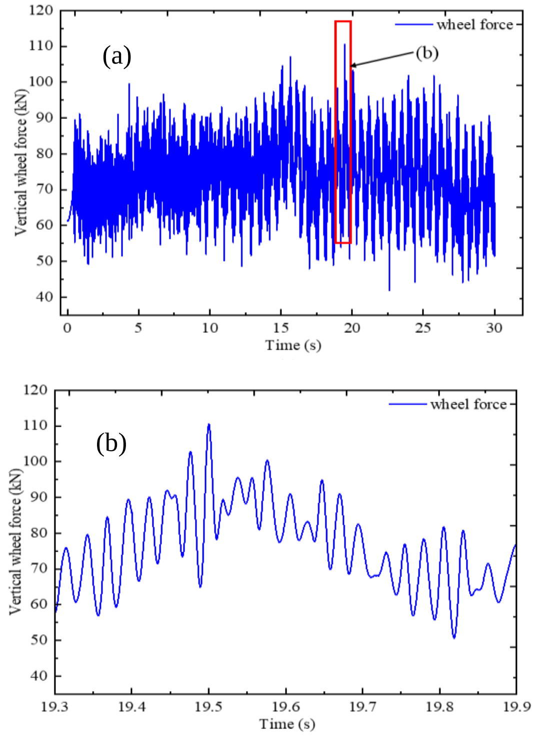

Fig. 4. (a) Vertical wheel force due to passengers' weight and (b) maximum vertical wheel force.

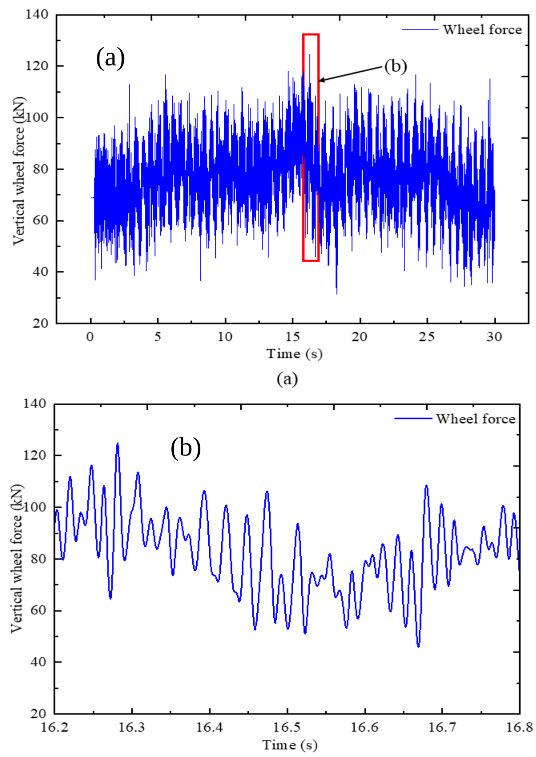

Fig. 5. (a) Vertical wheel force due to suspension system and (b) maximum vertical wheel force.

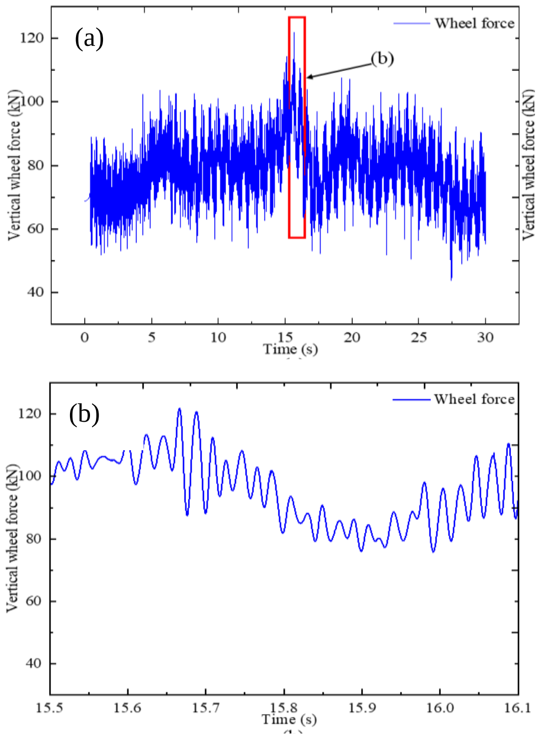

Fig. 6. (a) Vertical wheel force due to train speed and (b) maximum vertical wheel force.

Table 6 shows that the random suspension stiffness system has high maximum vertical wheel force (124.8kN) compared to random passenger weight and train speed. When the random suspension stiffness system results in a high maximum vertical wheel force compared to random passenger weight and train speed, it implies that the stiffness of the suspension system in the rolling stock is relatively high or stiff. This condition can have several implications when ride harshness, high dynamic loads, noise, and vibration increase, and passenger comfort reduces.

4.2. Finite element analysis

Stress, total deformation, and strain analysis obtained from FE analysis after applying the maximum vertical wheel force to the wheel are shown in Figs. 7-9 and tabulated in Table 7. The results show that case 2 has high equivalent stress compared to other cases.

4.3 Fatigue life analysis

The analysis of fatigue life was done by nCode software, and results are shown in Figs. 10, 11. The obtained fatigue life are tabulated in Table 7, and the results show that Case 2 has low life cycles compared to Case 1 and Case 3. The results obtained are similar to the findings reported by Zulkifli *et al.* [26], Mehmet et al. [25], Zhao *et al.* [24] and Aalami *et al.* [27]. The random parameters of the suspension system have more negative effects on fatigue life compared to random passengers' weight and train speed; this implies that variations and uncertainties in the suspension system play a more significant role in causing fatigue-related issues in the rolling stock. Here are some potential reasons for this scenario: design sensitivity, inadequate damping, component wear tear, maintenance challenge, inadequate quality control, insufficient design margin, and dynamic loading or environmental factors.

Table 6. Maximum vertical wheel force.

Maximum wheel force	Case 1	Case 2	Case 3
Vertical right (kN)	110.6	124.8	121.8

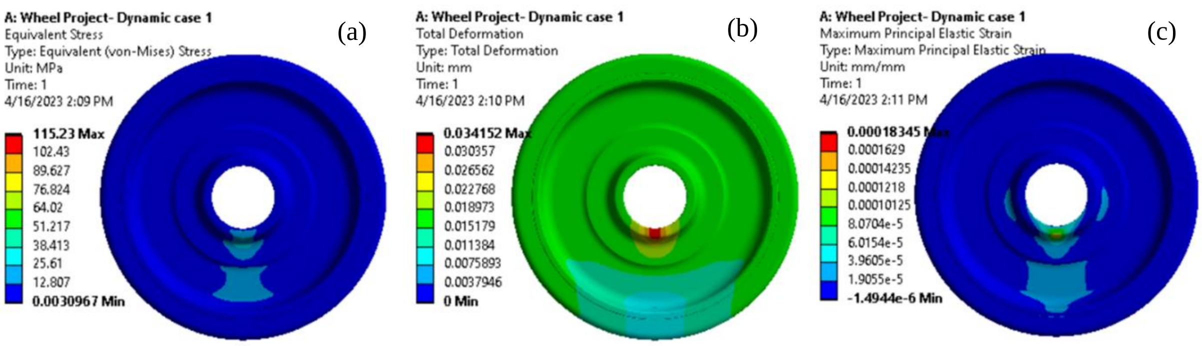

Fig. 7. Dynamic response due to passengers' weight (a) von-mises stress distributed in the wheel, (b) total deformation, and (c) maximum principal elastic strain.

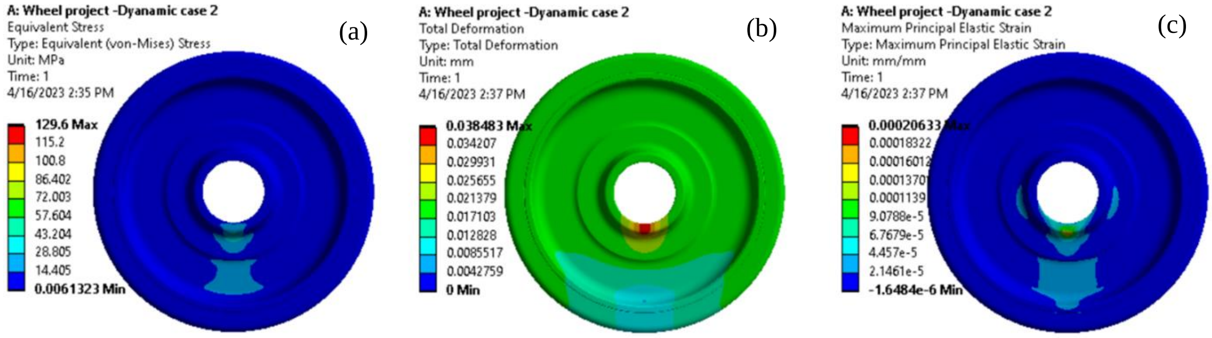

Fig. 8. Dynamic response due to random suspension system (a) von-mises stress distributed in the wheel, (b) total deformation, and (c) maximum principal elastic strain.

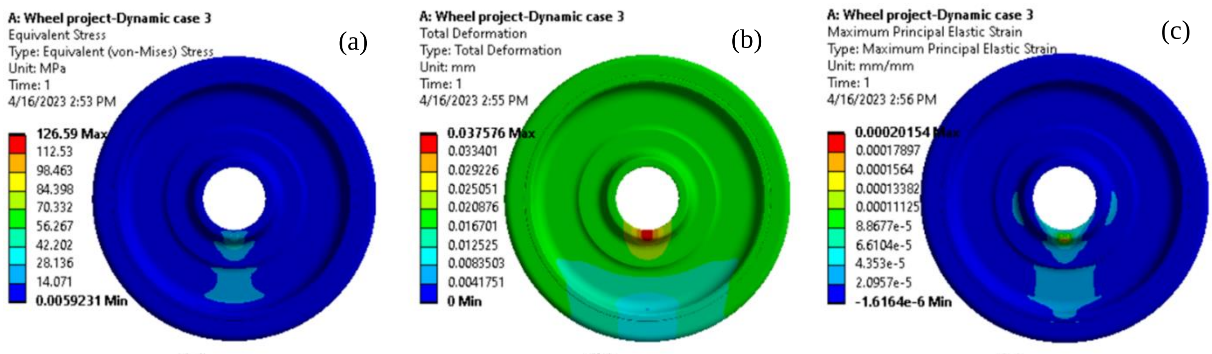

Fig. 9. Dynamic response due to random train speed (a) von-mises stress distributed in the wheel, (b) total deformation, and (c) maximum principal elastic strain.

Table 7. Finite element and nCode dynamic summarized results.

Cases	Equivalent stress (MPa)	Total deformation(mm)	Strain (mm/mm)	Damage	Fatigue life (N_f)
1	115.23	0.034152	0.00018345	1.591×10^{-9}	6.287×10^{8}
2	129.6	0.038483	0.00020633	3.5×10^{-9}	2.857×10^{8}
3	126.59	0.037576	0.00020154	2.99×10^{-9}	3.345×10^{8}

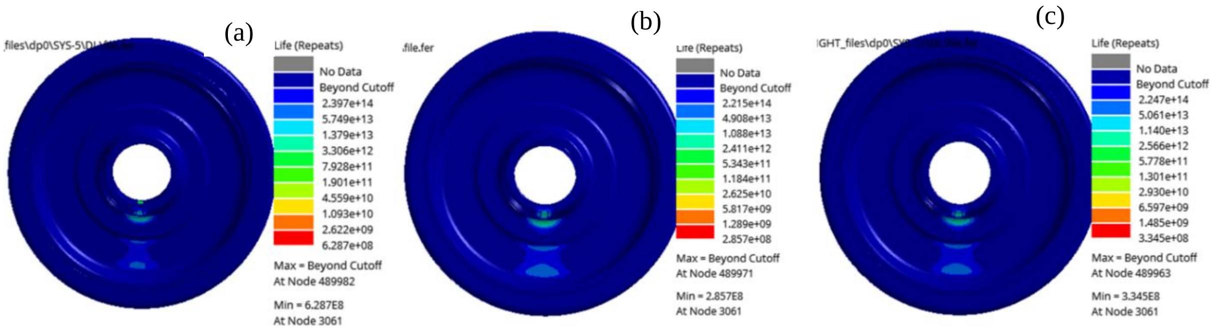

Fig. 10. Life cycles (a) due to passengers' weight, (b) due to random suspension system, and (c) due to random train speed.

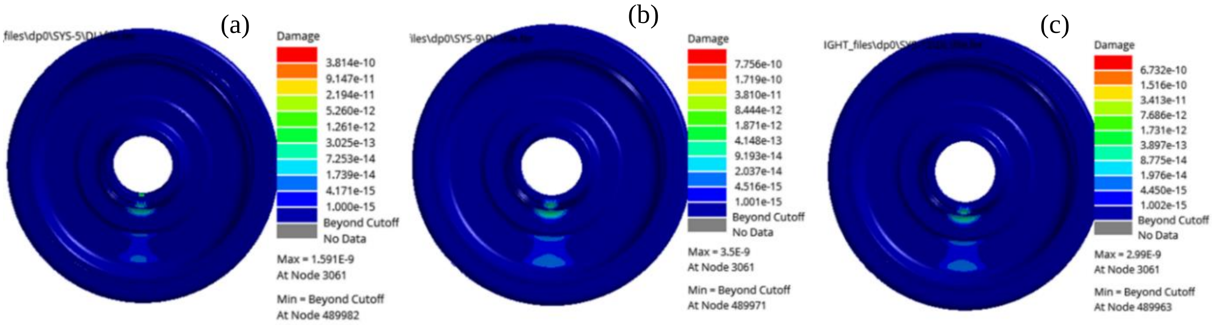

Fig. 11. Damage (a) due to passengers' weight, (b) due to random suspension system, and (c) due to random train speed.

5. Conclusions

The approach method used in this study, can inform decisions related to track maintenance, design improvements, and safety enhancements in rail transportation. Additionally, it can contribute to optimize railway operations and minimizing wear and tear on track infrastructure. The following conclusion was drawn:

(1) Through fatigue life analysis, it was determined that the random parameters of the suspension system have a more significant negative impact on fatigue life compared to random passengers' weight. This implies that variations in the suspension system characteristics have a greater influence on the components' durability. In addition, it states that random passengers' weight has less negative impact compared to the combined effect of random suspension and passengers' weight. This implies that while passengers' weight variations affect fatigue life, they are less influential when considered alongside variations in the suspension system.
(2) According to dynamic stress analysis, it was determined that the random suspension system parameters have high maximum stress compared to stress obtained from random passengers' weight and train speed.
(3) The random suspension system was obtained to have high maximum vertical wheel force compared to the maximum vertical wheel force obtained due to random passengers' weight and train speed.
(4) The random suspension system was obtained a higher total deformation and strain effect on the wheel compared to the total deformation and strain effect obtained due to random passengers' weight and train speed.
According to the findings, studying the fatigue life of railway wheels is essential for ensuring the safety, reliability, and cost-effectiveness of rail transportation. It plays a critical role in preventing accidents, reducing maintenance costs, and optimizing the performance of rail systems, benefiting both passengers and the industry as a whole.

Conflict of interest's declaration

The authors assert that there are no prevailing conflicts of interest in connection with this manuscript, encompassing the study, authorship or publication.

Acknowledgments

The authors would like to express their heartfelt gratitude to the World Bank (WB) for their invaluable support in facilitating the railway engineering courses at African Railway Center of Excellence (ARCE), Addis Ababa University. This support has played a pivotal role in advancing our educational and research endeavors, contributing significantly to the development of railway expertise in our region.

References

[1] Q. Zhang, I. T. Caraballo, Q. Li, J. Han, J. Han, J. Zhao and G. Dai, "Tension-shear multiaxial fatigue damage behavior

of high-speed railway wheel rim steel," *Int. J. Fatigue*, Vol. 133, p. 105416, (2020),

[2] Q. Y. Xiong, S. T. Yu, and J. S. Ju, "Fatigue analysis on wheel considering contact effect using FEM method," *Math. Probl. Eng.*, Vol. 2015, (2015).

[3] Q. Xiao, J. Zheng, J. Liu, and J. Fang, "Analysis of the wheel/rail rolling contact fatigue of a high-speed train under the transient mechanism," *J. Mech. Sci. Technol.*, Vol. 31, No. 5, pp. 2235–2242, (2017).

[4] J. Luo, S. Wang, X. Liu, and S. Geng, "Fatigue life prediction of train wheel shaft based on load spectrum characteristics," *Adv. Mech. Eng.*, Vol. 13, No. 2, pp. 1–10, (2021).

[5] W. Jianxi, G. Jirong, C. Long, and L. Xiangguo, "Distribution characteristics of wheel–rail contact under random parameters," *Aust. J. Mech. Eng.*, Vol. 17, No. 3, pp. 155–161, (2019).

[6] Y. Lu, Y. Yang, J. Wang, and B. Zhu, "Optimization and Design of a Railway Wheel Profile Based on Interval Uncertainty to Reduce Circular Wear," Vol. 12, p. 9579510, (2020).

[7] A. Ekberg, *Fatigue of railway wheels*. Woodhead Publishing Limited, (2009).

[8] R. Masoudi Nejad and F. Berto, "Fatigue fracture and fatigue life assessment of railway wheel using non-linear model for fatigue crack growth," *Int. J. Fatigue*, Vol. 153, No. September, pp. 10–13, (2021).

[9] X. Zhao, Z. Wang, Z. Wen, H. Wang, and D. Zeng, "The initiation of local rolling contact fatigue on railway wheels: An experimental study," *Int. J. Fatigue*, Vol. 132, No. July, p. 105354, (2020).

[10] D. Zhou and J. Chang, "Fatigue Analysis of a Light Truck Rear Axle Based on Virtual Iteration Method," *Shock Vib.*, Vol. 21, p. 8598491, (2022).

[11] S. A. Snitko, A. V. Yakovchenko, and S. M. Gorbatyuk, "Accounting method for residual technological stresses in modeling the stress-deformed state of a railway wheel disk. Report 2," *Izv. Ferr. Metall.*, Vol. 64, No. 7, pp. 477–483, (2021).

[12] Z. A. Soomro, "Calculation of lateral velocity estimation and error discrimination for railway wheelset to avoid sliding," *J. Comput. Appl. Res. Mech. Eng.*, Vol. 8, No. 2, pp. 145–151, (2019).

[13] M. Asplund, M. Palo, S. Famurewa, and M. Rantatalo, "A study of railway wheel profile parameters used as indicators of an increased risk of wheel defects," *Proc. Inst. Mech. Eng. Part F J. Rail Rapid Transit*, Vol. 230, No. 2, pp. 323–334, (2016).

[14] O. Polach and D. Nicklisch, "Wheel/rail contact geometry parameters in regard to vehicle behaviour and their alteration with wear," *Wear*, Vol. 366–367, pp. 200–208, (2016).

[15] A. Haidari and P. Hosseini-Tehrani, "Fatigue analysis of railway wheels under combined thermal and mechanical loads," *J. Therm. Stress.*, Vol. 37, No. 1, pp. 34–50, (2014).

[16] X. Huang, X. Wang, X. Shen, and F. Xiao, "Effect of the shape of railway wheel plate on its stresses and fatigue evaluation," *Eng. Fail. Anal.*, Vol. 97, No. December 2017, pp. 718–726, (2019).

[17] R. Masoudi Nejad and F. Berto, "Fatigue fracture and fatigue life assessment of railway wheel using non-linear model for fatigue crack growth," *Int. J. Fatigue*, Vol. 153, No. August, p. 106516, (2021).

[18] T. A. Zucarelli, M. A. Vieira, L. A. Moreira Filho, D. A. P. Reis, and L. Reis, "Failure analysis in railway wheels," *Procedia Struct. Integr.*, Vol. 1, pp. 212–217, (2016).

[19] R. Masoudi Nejad and F. Berto, "Fatigue crack growth of a railway wheel steel and fatigue life prediction under spectrum loading conditions," *Int. J. Fatigue*, Vol. 157, No. April, pp. 1–4, (2022).

[20] Q. Zhang, I. Toda-Caraballo, G. Dai, Z. Feng, Q. Li, and D. Yu, "Influence of laminar plasma quenching on rolling contact fatigue behaviour of high-speed

railway wheel steel," *Int. J. Fatigue*, Vol. 137, No. April, p. 105668, (2020).

[21] M. Yamamoto, "Non-parametric optimization of railway wheel web shape based on fatigue design criteria," *Int. J. Fatigue*, Vol. 134, p. 105463, (2020).

[22] T. Jia, Z. Shen, C. Liu, X. Zhao, and X. Zhang, "Study on Mechanism and Influencing Factors of Wheel Strengthening and Toughening of High-Speed and Heavy-Load Train," *Crystals*, Vol. 13, No. 1, pp. 1–11, (2023).

[23] Y. Hu, Z. Hu, and S. Cao, "Theoretical study on Manson-Coffin equation for physically short cracks and lifetime prediction," *Sci. China Technol. Sci.*, Vol. 55, No. 1, pp. 34–42, (2012).

[24] X. Zhao, Z. Wen, M. Zhu, and X. Jin, "A study on high-speed rolling contact between a wheel and a contaminated rail," *Veh. Syst. Dyn.*, Vol. 52, No. 10, pp. 1270–1287, (2014).

[25] M. A. Arslan and O. Kayabaşi, "3-D Rail-Wheel contact analysis using FEA," *Adv. Eng. Softw.*, Vol. 45, No. 1, pp. 325–331, (2012).

[26] M. A. Che Zulkifli, K. S. Basaruddin, M. Afendi, W. H. Tan, and E. M. Cheng, "Finite Element Simulation on Railway Wheels under Various Loading," *IOP Conf. Ser. Mater. Sci. Eng.*, Vol. 429, No. 1, (2018).

[27] M. R. Aalami, A. Anari, T. Shafighfard, and S. Talatahari, "A robust finite element analysis of the Rail-Wheel rolling contact," *Adv. Mech. Eng.*, Vol. 2013, p. 272350, (2013).

[28] J. Sandström, "Subsurface rolling contact fatigue damage of railway wheels - A probabilistic analysis," *Int. J. Fatigue*, Vol. 37, pp. 146–152, (2012).

[29] A. Momhur, Y. X. Zhao, W. Q. Li, Y. Z. Sun, and X. L. Zou, "Flexible-Rigid Wheelset Introduced Dynamic Effects due to Wheel Tread Flat," *Shock Vib.*, Vol. 2021, pp. 13–23, (2021).

[30] Y. Hu, M. watson, M. Maiorino, L. Zhou,W. J. Wang, H. H. Ding, R. Lewis, E. Meli, A. Rindi, Q. Y. Liu and J. Guo, "Experimental study on wear properties of wheel and rail materials with different hardness values," *Wear*, Vol. 477, No. February, p. 203831, (2021).

[31] Q. An, H. Zhao, P. Li, and M. Fu, "Fatigue strength analysis of bogie frames under random loads," *Adv. Mech. Eng.*, Vol. 11, No. 9, pp. 1–13, (2019).

[32] Y. Yang, L. Ling, J. Wang, and W. Zhai, "A numerical study on tread wear and fatigue damage of railway wheels subjected to anti-slip control," *Friction*, (2023).

[33] J. Pombo, J. Ambrosio, M. Pereira, R. Lewis, R. Dwyer-Joyce, C. Ariaudo and N. Kuka, "A study on wear evaluation of railway wheels based on multibody dynamics and wear computation," *Multibody Syst. Dyn.*, Vol. 24, No. 3, pp. 347–366, (2010).

[34] J. J. Kalker, "Survey of Wheel-Rail Rolling Contact Theory," *Dyn. Veh. roads tracks*, May 2013, pp. 13–13, (2018).

[35] Z. Yang and Z. Li, "Wheel-rail dynamic interaction," *Rail Infrastruct. Resil. A Best-Practices Handb.*, January, pp. 111–135, (2022).

[36] X. Wang, J. Zhang, and J. Zuo, "Wheel Tread Wear Prediction of High-Speed Railway Train," *Tribol. Lett.*, Vol. 70, No. 2, pp. 1–10, (2022).

[37] B. Peng, S. Iwnicki, P. Shackleton, and Y. Song, "General conditions for railway wheel polygonal wear to evolve," *Veh. Syst. Dyn.*, Vol. 59, No. 4, pp. 568–587, (2021).

[38] M. N. Tawfik, M. M. Padzi, Shahrum, H. Hapaz, M. Zahar, and M. Nur Firdaws, "Approaches of Finite Element Analysis to Study Fatigue Analysis of Rail-Wheel Contact for Light Rail Transit," *Int. J. Integr. Eng.*, Vol. 14, No. 8, pp. 86–91, (2022).

[39] A.Cera 1 , G.Mancini 1 , V.Leonardi 1 , L.Bertini "Analysis of methodologies for fatigue calculation for railway bogie frames.," (2006).

[40] T. Y. Kim and H. K. Kim, "Three-dimensional elastic-plastic finite element analysis for wheel-rail rolling contact

fatigue," *Int. J. Eng. Technol.*, Vol. 6, No. 3, pp. 1593–1600, (2014).

[41] B. Jagadeep, P. Kiran Kumar, and K. V. Subbaiah, "Stress Analysis on Rail Wheel Contact," *Int. J. Res. Eng.*, No. 1, pp. 47–52, (2018), [Online]. Available: www.ijresm.com

[42] H. M. El-sayed, M. Lotfy, H. N. El-din Zohny, and H. S. Riad, "Prediction of fatigue crack initiation life in railheads using finite element analysis," *Ain Shams Eng. J.*, Vol. 9, No. 4, pp. 2329 – 2342, (2018).

[43] J. P. Srivastava, P. K. Sarkar, and V. Ranjan, "Contact Stress Analysis in Wheel–Rail by Hertzian Method and Finite Element Method," *J. Inst. Eng. Ser. C*, Vol. 95, No. 4, pp. 319–325, (2014).

How to cite this paper:

Mazuri Erasto Lutema and Awel Mohammedseid Momhur, " Fatigue analysis of CRH2 high speed train railway wheels occurred due to random parameters,", *J. Comput. Appl. Res. Mech. Eng.*, Vol. 13, No. 2, pp. 207-218, (2024).

DOI: 10.22061/JCARME.2023.9754.2315

URL: https://jcarme.sru.ac.ir/?_action=showPDF&article=1995